

What Control Segmentations of Mega-Thrust Earthquakes in the Nankai Seismogenic Zone: a Review of High-Resolution Wide-Angle Seismic Surveys

Shuichi Kodaira^{1)*}, Ayako Nakanishi¹⁾, Jin-Oh Park¹⁾, Narumi Takahashi²⁾ and Yoshiyuki Kaneda¹⁾

¹⁾ Institute for Frontier Research on Earth Evolution, Japan Marine Science and Technology Center

²⁾ Deep Sea Research Department, Japan Marine Science and Technology Center

Abstract

A series of wide-angle seismic surveys has been carried out in recent years of the entire Nankai seismogenic zone under the working hypothesis, “structure of subducted plate might control segmentation of rupture zones”. In this paper we summarize the key results of these surveys. Along a profile crossing the rupture zone of the 1946 Nankaido earthquake we successfully imaged a large-scale subducted seamount, which is 50 km wide and 3 km high. The seamount is interpreted to be one member of the Kinan seamount chain, which is recognized on the incoming plate. Comparing the location of the subducted seamount and a detailed rupture distribution of the 1946 event shows that the rupture starting off Cape Shiono turned around the landward foot of the seamount. Another structure preventing rupture propagation was also found along a profile looking at the eastern edge of the 1944 Tonankai earthquake. High-resolution wide-angle seismic data clearly imaged two lines of subducted ridges, which are interpreted to be a subducted ridge parallel to the present day ridge system on the incoming plate. One of the subducted ridges is situated immediately outside the rupture zone where GPS data indicate strong coupling at present. We propose, from these results, that a subducted convex, which underlays a back stop structure, played the role of a barrier preventing earthquake rupture propagation.

Key words: Nankai trough, seismic survey, seismogenic zone, oceanic crust, subduction

1. Introduction

Several geophysical studies have suggested possible candidates of structural factors controlling lateral extensions of the co-seismic rupture zones and inter-plate locked zones, e.g., amount of sediments between plates (Ruff, 1989), roughness of subducting plate (Kelleher and McCann, 1976; Scholz and Small, 1997), and anelasticity in a weak zone at an upper plate (MaCaffrey, 1993). However, decisive evidence showing a direct relationship between a structure and an earthquake rupture process has not been well demonstrated due to a lack of detailed structural images with sufficient resolution.

The Nankai trough is one of the best experimental sites among the world's subduction zones for investigating structural factors controlling the lateral extension of rupture zones. The segmentation of rupture zones and the recurrence intervals of magnitude class eight earthquakes are well-documented on the basis of geophysical, geological, and historic data (e.g., Sangawa, 1998, Ando, 1975 b). According to historic data, as well as available seismological data, all four segments shown in Fig. 1 have slipped five times at regular intervals (90–150 years) since 1605 in one or two successive events, except for the western most segment (segment D in Fig. 1, hereafter, re-

* e-mail: kodaira@jamstec.go.jp (3173-25, Showa-machi, Kanazawa-ku, Yokohama, 236-0001 Japan)

ferred to as the Tokai segment) [Ando, 1975 b].

Concerning rupture segmentation of the 1946 Nankaido earthquake, two conflicting results are derived independently from seismic data and geodetic data. The geodetic data show a rupture area of $2.5 \times 10^4 \text{ km}^2$, with a slip of 5–18 m [Fitch and Scholz, 1971] (segments A and B), while the seismic data show a rupture area of $1 \times 10^4 \text{ km}^2$ with a slip of 3 m [Kanamori, 1972] (segment B). The most recent tsunami wave inversion suggests that the rupture extended near the deformation front in segment B, while the rupture in segment A only propagated along the deep portion [Baba *et al.*, 2002].

The last earthquake rupture at the Tokai segment occurred in 1854, but a slip during the 1944 Tonankai earthquake did not extend into this segment (Fig. 1) [Ando, 1975 b; Tanioka and Satake,

2001; Kikuchi and Yamanaka, 2001]. A recent report also states that ruptures during the historical great earthquakes have not always extended to the entire Tokai segment [Earthquake research committee, 2001]. Based on these data several studies proposed a future large earthquake in this non-ruptured segment [Ando, 1975 a; Ishibashi, 1976], however, there are still arguments for and against the possibility of a future great earthquake in the Tokai segment [Ishibashi, 1976; Geller, 1997]. The seismological data also indicate that earthquake ruptures have started off Cape Shiono between segments B and C at least in the last two earthquakes.

In recent years we carried out a series of wide-angle seismic surveys in the entire Nankai seismogenic zone under the working hypothesis, “structure of subducted plate might control segmentation of

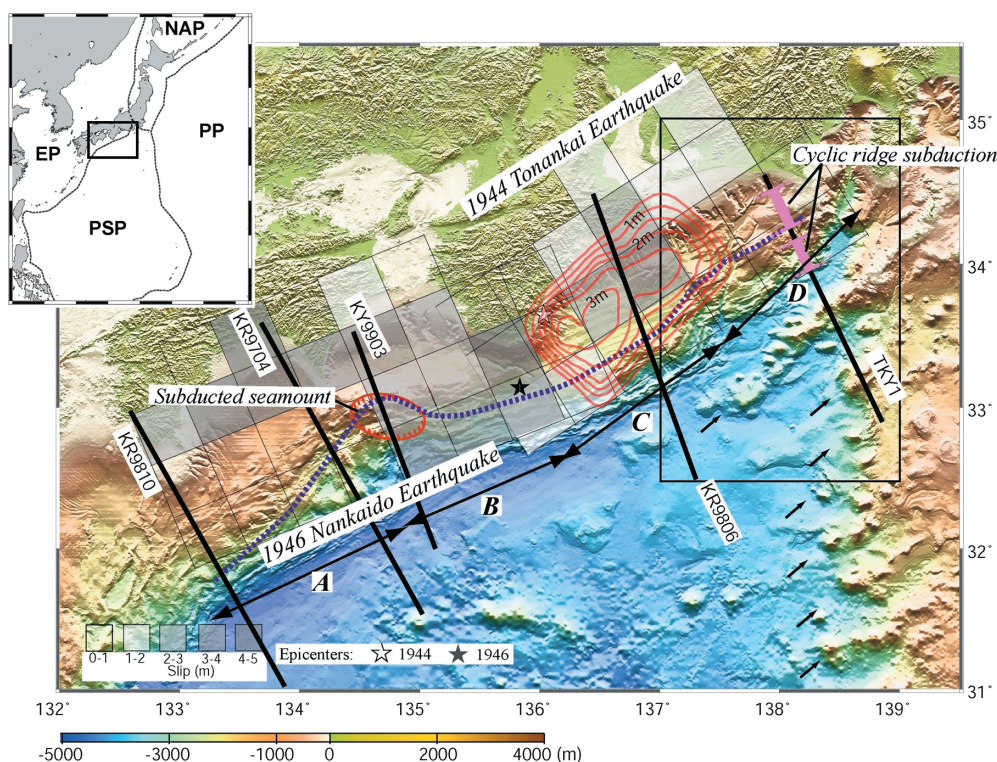


Fig. 1. Topography of the Nankai trough and location of wide-angle seismic profiles (bold lines). The four segments of rupture zones A to D compiled from historical earthquake data are shown [Ando, 1975b]. Gray squares show rupture zones during the 1944 Tonankai earthquake [Tanioka and Satake, 2001] and 1946 Nankai earthquake [Bbta *et al.*, in press] estimated from tsunami wave data. Red contours show co-seismic slip during the 1944 Tonankai earthquake estimated from near field strong ground motion data [Kikuchi and Yamanaka, 2001]. These rupture zones clearly demonstrate that the rupture did not extend to the Tokai segment. Locations of a subducted seamount off Shikoku island [Kodaira *et al.*, 2000 a], a subducted ridges off Tokai [Kodaira *et al.*, 2003], and the seaward end of the back stop accumulating sediments from the incoming plate [Nakanishi *et al.*, 2002 d] are plotted. Arrows indicate sub-parallel volcanic ridges on the incoming plate [Ishizuka *et al.*, 1998; Le Pichon *et al.*, 1996]. Framed area is enlarged in Fig. 6. Bathymetry data were compiled by the Hydrographic Department, Japan Maritime Safety Agency. NAP, North American plate; PP, Pacific plate; EP, Eurasian plate; PSP, Philippine Sea plate.

rupture zones”.

In this paper we summarize the key results of the wide-angle seismic surveys mainly focusing two high-resolution surveys [Kodaira *et al.* 2000 a, Kodaira *et al.* 2003], and discuss the implications for relations between the structures and the rupture segmentations.

2. Overall structure and its tectonic implications

From results of wide-angle seismic surveys carried out in recent years, [Research group for explosion south off Kii peninsula 1995, Nishisaka *et al.*

1996, Nishisaka *et al.* 1997, Nakanishi *et al.* 1998, Kodaira *et al.* 2000 a, Kodaira *et al.* 2000 b, Kodaira *et al.* 2002, Nakanishi *et al.* 2002 a, Nakanishi *et al.* 2002 b, Nakanishi *et al.* 2002 c, Takahashi *et al.*, 2002, Kodaira *et al.*, 2003], it is recognized that the subduction structure consists of three distinct structures (Fig. 2): 1) subducting oceanic crust, 2) sedimentary wedge beneath the continental slope, and 3) crustal block immediately landward of the sedimentary wedge.

According to the distribution of the geotectonic unit [Taira *et al.* 1992], the sedimentary wedge can be interpreted to be the Neogene-Quaternary accretion-

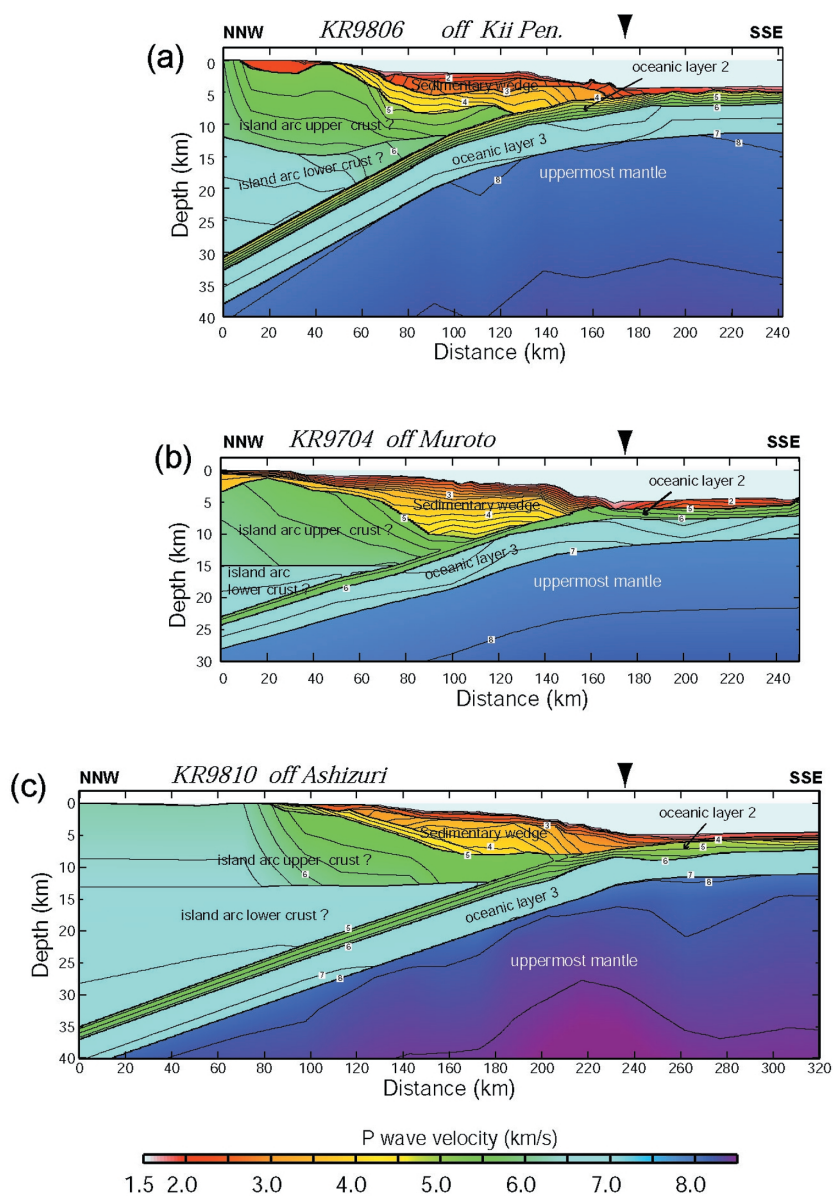


Fig. 2. Overall structure of the Nankai subduction zone obtained by conventional wide-angle seismic surveys. (a) off the Kii peninsula (KR9806 in Fig. 1) after Nakanishi *et al.* [2002 b]. (b) off the cape Muroto (KR9704) after Kodaira *et al.* [2000 b]. (c) off the cape Ashizuri (KR9810) after Takahashi *et al.* [2002].

ary prism [e.g. Nakanishi *et al.* 2002 b]. Velocity of the crustal block landward of the sedimentary wedge is higher than that of the overlying Neogene-Quaternary accretionary prism. Older sedimentary rocks are usually considered to have a higher velocity due to compaction and alteration [e.g. Davidson *et al.* 1997]. From a geological point of view, the entire area of the southwestern Japan is predominantly formed by active sedimentary accretion, which is considered to be an important mechanism of the crustal growth of the Japanese Island arc [Taira *et al.* 1987].

The crustal block can be interpreted as the Cretaceous-Tertiary accretionary prism [e.g. Nakanishi *et al.* 2002 b, Kodaira *et al.* 2000 b], formed before the opening of the Shikoku Basin [e.g. Nakanishi *et al.* 2002 c]. We will, therefore, refer to this crustal block as crustal block of old accreted sediments. Although the expression is not appropriate, this crustal block sometimes has been referred to Island arc upper crust [e.g. Nakanishi *et al.* 1998]. The Kula-Pacific plate is proposed to have been subducting north-westward beneath southwest Japan in the Paleogene on the basis of magnetic anomalies and stress orientation of the structural fabric of the early Tertiary Shimanto Belt [Byern and Ditullio, 1992]. The crustal block of old accreted sediments is likely to be accreted during subduction of the Kula-Pacific plate before the opening of the Shikoku Basin. Although differences in geological structure cannot be directly resolved in our crustal models, the northwestward increase in the velocity of the crustal block of old accreted sediments may indicate that metamorphic grade changes northwestwards.

3. Structures controlling segmentations of the rupture zones

3-1. Subducted seamount between segments A and B

Data acquisition and processing: a high-resolution deep seismic study has been performed in the middle of the proposed rupture zone of the Nankaido earthquake (Fig. 1). The profile is designed to be located at the western edge of the 1-day after-shock area [Mogi 1968]. To resolve the seismic velocity structure with high resolution to 10–30 km in depth, 98 Ocean bottom seismographs (OBSs) were deployed with a spacing of 1.6 km on the 185 km long profile, and a large

air-gun array (12,000 cu. inch) was fired at every 200 m. This spacing of the OBSs is more than ten times closer than that of a conventional seismic refraction survey. All OBSs were positioned at the sea bottom using a super short base line (SSBL) acoustic positioning system.

All observed record sections showed first arrivals (P-wave refraction arrivals) throughout the entire profile, except for OBSs deployed in shallow water (water depth of less than 200 m). The observed data yielded 44,517 first arrival picks, from which we determined the P-wave velocity (V_p) structure with seismic refraction tomography [Zelt and Barton 1998]. A model was parameterized in 0.5×0.5 km cells. We used a simple landward dipping structure as the starting model, based on a recent model of the Nankai Trough [Kodaira *et al.*, 2000 b]. The root-mean-square (RMS) of the travel time residual calculated from the starting model is 2.4 s, while after tomographic inversion the final model shows that the RMS residual is reduced to 0.1 s, which is comparable to the uncertainty for travel time data (0.02–0.10 s).

Seismic velocity image: The final seismic velocity image (Fig. 3) shows two significant structures, i) a thick $V_p=5.0\text{--}7.2$ km/s body at the middle of the profile 25 km seaward from the Tosa-bae topographic high and ii) structure with $V_p=5.0\text{--}6.0$ km/s, which becomes shallower toward the landward end of the profile. The thickness and the width of the $V_p=5.0\text{--}7.2$ km/s body are 7–13 km and 50 km wide, respectively, and it thins to 6 km on either side. According to previous conventional seismic refraction studies at the northern edge of the Philippine Sea plate [e.g., Kodaira *et al.*, 2000 b] P-wave velocities of the oceanic crust range between 5.0 and 7.0 km/s with a thickness of 6 km. The thick 5.0–7.2 km/s body at the middle of the model may be locally thickened oceanic crust. Seismic reflection data acquired over the thick $V_p=5.0\text{--}7.2$ km/s body show that the top of the oceanic crust rises 1–2 km at the seaward side of the Tosa-bae. The top of the oceanic crust interpreted from the seismic reflection data is plotted on our velocity model. From these seismic data, we infer that our seismic data imaged a large-scale subducted seamount (50 km wide and 13 km thick). This conclusion is supported by: i) the existence of the Kinan seamount along the southeastern extension of our

profile [Kobayashi *et al.*, 1995], ii) a magnetic study [Yamazaki and Okamura, 1989], which suggests the possibility of a subducted seamount near the Tosa-bae and iii) a landward indentation of the topography recognized seaward of the Tosa-bae, [Yamazaki and Okamura, 1989]. The shape of this indentation agrees with that obtained from analog modeling of seamount subduction beneath an accretionary prism [Domingues *et al.*, 1998]. The other significant structure, a region having $V_p=5.0\text{--}6.0$ km/s that thickens to landward, is interpreted to be the Japanese island arc upper crust consisting of old accretionary material. Previous seismic refraction studies [e.g. Kodaira *et al.*, 2000 b] near the Nankai Trough also indicate landward thickening of the Japanese island arc upper crust.

The number of rays running through cells of the model is considered to be an index of the reliability

of the model. Both features of the velocity structure lie within regions with good ray coverage (Fig. 3 b) and these features are well resolved. The only areas not well constrained by the data are small areas at the western edge and the deepest part of the model. Thus, the model (Fig. 3) resolves a subducted seamount in contact with the Japanese island arc upper crust beneath the Tosa-bae at 10 km depth. We conclude from this result that the seamount is currently colliding with the island arc.

3-2. Cyclic ridge subduction in segment D

Data acquisition and processing: We designed an integrated seismic profile at the edge of the rupture zone of the Tonankai earthquake (Fig. 1). The seismic data used were deep penetrating seismic refraction/wide-angle reflection waves combined with near vertical reflection waves. Because we aimed to obtain a high resolution seismic image into inter-

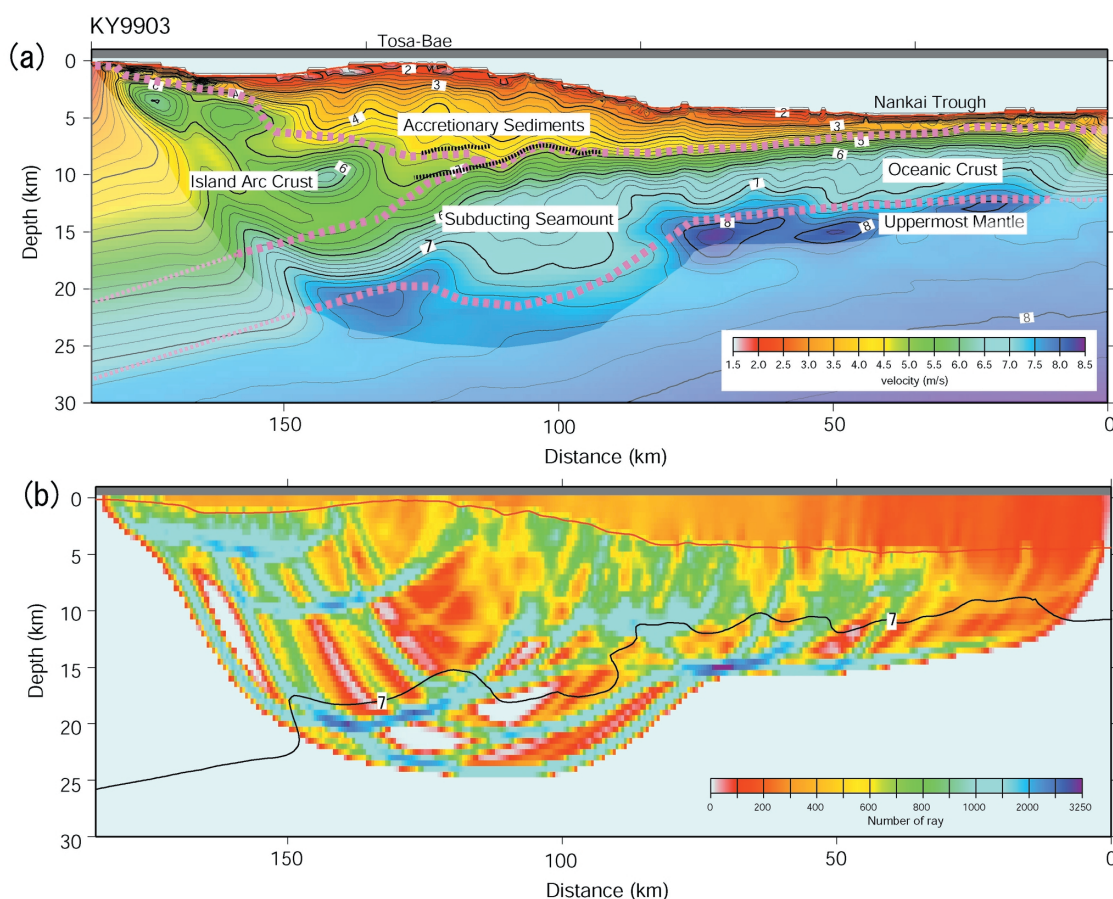


Fig. 3. (a) Seismic velocity image off east of the Cape Muroto (KY9903) obtained by a high-resolution wide-angle seismic survey [Kodaira *et al.* 2000 a]. Contour interval is $V_p=0.5$ km/s. Lighter colored regions show no seismic ray sampled. Geological interpretation is superimposed. Dotted lines beneath the Tosa-bae represent interfaces interpreted from seismic reflection data, i.e., an intra-crustal reflector (top) and the top of the oceanic crust (bottom). (b) Number of rays running in each cell (0.5×0.5 km). An iso-velocity contour of 7 km/s is superimposed.

plate locked zone, which was expected 10–20 km depth [Sagiya, 1999], we also used a super-densely deployed OBS array, while the OBS spacing was slightly larger than that of the previous experiment (i.e., 70 OBSs with a spacing of 3 km on the 215 km profile). The same large air-gun array (12,000 cu. inch) was used.

Figure 4 shows an example of the observed wide-angle seismic data, with plotted offset distances of less than 100 km at the southeastern side of Site 16 (Fig. 5). The refraction arrivals are often traced up to 200 km offset on the several OBSs. These large offset refraction arrival data were necessary to resolve a deeper part of a seismic velocity image (Fig. 5 a). Wide-angle reflection phases from the base of the crust (Moho), as well as reflections within the crust, are also clearly observed (Fig. 4). These reflection phases were used to create a seismic reflectivity image (Fig. 5 b).

The modeling method applied to the first arrival data is the same as the above, seismic refraction tomography [Zelt and Barton, 1998]. We used a simplified structure from results of a previous seismic refraction study [Nakanishi *et al.*, 1998]. Root mean square (RMS) of the travel time residual calculated from the starting model is 0.68 s, while after tomographic inversion, the final model shows the RMS converged down to 0.09 s. Because the first arrival tomography does not reveal a reflector image, we also applied pre-stack depth migration (PSDM), which is widely used for processing near vertical seismic reflection (multichannel seismic reflection)

data, to the wide-angle seismic data. PSDM enables the use of higher amplitude wide-angle (post critical) reflection phases and a precise velocity structure, which is necessary for the migration, and can be obtained prior to the migration by the tomographic approach [Zelt, *et al.*, 1998].

Seismic velocity and reflectivity images: Figs. 5 a and 5 b show the seismic velocity and reflectivity images, respectively. In Fig. 5 b, a seismic reflection section from the near vertical reflection data is super-imposed to show a higher resolution image at the shallower part (shallower than 14 km in depth at the middle of the profile). Generally, the near vertical seismic reflection data provide a higher resolution structure for a shallow region, while the reflectivity images from the wide-angle reflection data provide a deeper image (e.g. down to a base of a crust), even though it is with lower resolution. Reflectors picked up from the reflectivity image (Fig. 5 b) are plotted on the seismic velocity image (Fig. 5 a) with interpretations of the crustal block.

The most remarkable structure is the repeated crustal thickening with thicknesses of 13–20 km and wavelengths of 35–50 km shown as crustal blocks A to D in Fig. 5 a. This feature is clearly recognized from the shapes of iso-velocity contours in Fig. 5 a and the reflectors F and G in Fig. 5 b, i.e., the iso-velocity contour of 4–7 km/s shows repeated broader and narrower widths at 50, 100, 135, and 170 km on the model axis, and reflectors F and G show bulges at the same positions. Another key structure is overriding the crustal block D; i.e., the iso-velocity contours of

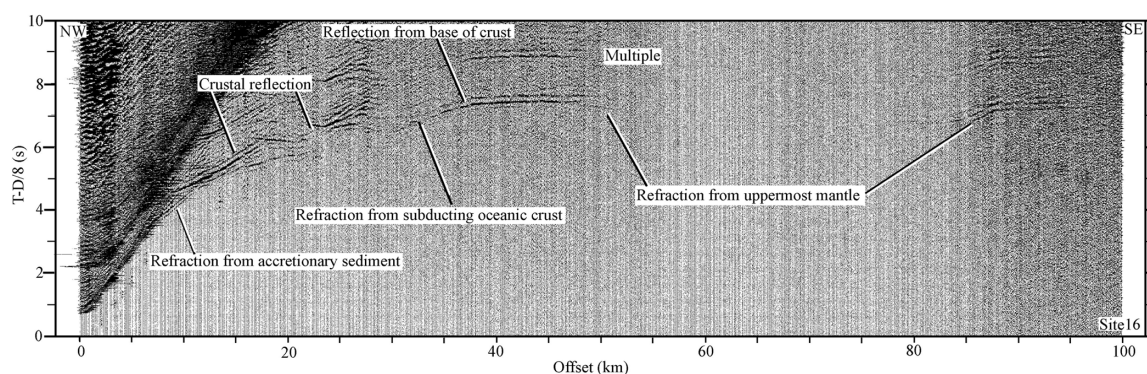


Fig. 4. An example of observed wide-angle seismic data acquired along TKY1 (Fig. 1) showing an offset distance of less than 100 km in Site 16 (see location in Fig. 5 a). The vertical axis represents travel times reduced by 8 km/s. Clear refraction first arrivals, as well as reflection phases, are observed. These phases are used to obtain a seismic velocity image and a reflectivity image, respectively. Band-pass filter (5–20 Hz) and predictive deconvolution filter are applied. Amplitudes are scaled proportionally to the square root of the offsets.

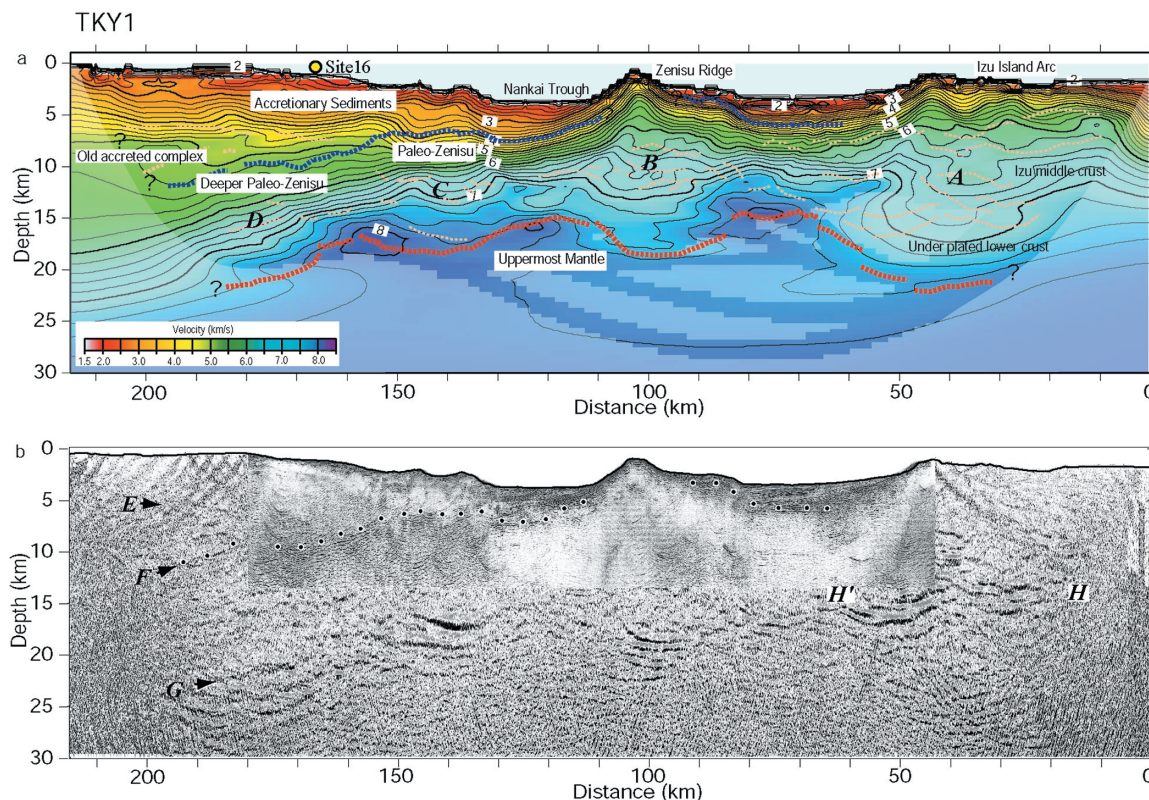


Fig. 5. Seismic velocity and reflectivity images off Tokai (TKY1) obtained by high-resolution wide-angle seismic survey [Kodaira *et al.* 2003]. (a) Seismic velocity image obtained from first arrival refraction tomography. Dotted lines indicate reflectors picked up from a seismic reflectivity image (Fig. 5b). Lighter colored regions shows no seismic ray sampled. The blue and red dotted lines indicate a top and bottom of an igneous crust. Repeated crustal thickening (labeled A to D) is observed. The crustal blocks A and B show structures of the western flank of the Izu arc including the Proto Zenisu ridge and the Zenisu ridge, respectively. The crustal blocks C and D indicate an ongoing cyclic ridge subduction at the Tokai segment. (b) Seismic reflectivity image obtained by pre-stack depth migration (PSDM) of wide-angle seismic data. Seismic reflectivity image from near vertical seismic data (conventional multi-channel reflection data) is superimposed at the middle of the section (shallower than 14 km between 45 km and 180 km on the model axis). Prior to PSDM, amplitude equalization of all receiver gathered data (OBS data), band-pass filter (5–20 Hz) and predictive deconvolution filter are applied. Reflectors labeled E, F, and G are interpreted as the top of an old accretionary complex, and the top and the bottom of an igneous crust, respectively. A reflector between H-H' is considered to be the top of the middle crust observed at the Izu arc. A weak reflector interpreted to be the bottom of the Izu arc crust is recognized at depths of 20–23 km between 30–60 km on the model axis. Note that striking bubble reverberations from the large (non-tuned) air-gun array remained especially at the deeper part.

4.5–5.5 km/s broaden toward the land above crustal block D. This landward thicker structure is bounded by the weak reflector E at the top. The reflectors labeled E, F, G, and H are interpreted as the top of an old accretionary complex, the top of the subducting crust, the base of the crust, and the reflectors at the top of the Izu middle crust, respectively. The reflector corresponding to the base of the crust is not well imaged at 0–50 km on the model axis, but we picked up the continuous weaker reflector at around 22 km in depth as the base of the crust beneath the western flank of the Izu arc.

4. Implications for segmentation of the rupture zone and conclusions

In segments A and B, recently a study of tsunami data from the 1946 Nankaido earthquake [Kato and Ando, 1997] recently showed a short rise time of the seismic wave in the 1-day after-shock area and slow slip (rise time of 3–9 min) in the area to the west of the after-shock zone. Cummins *et al.* [2000] and Cummins *et al.* [2002] also concluded that the earthquake rupture that generated short-period seismic waves is comparable to the 1-day aftershock areas and suggested that the slow slip occurred along a splay fault

cutting through the accretionary sediment to the west of Tosa-bae. From these two studies it could be proposed that two phases of the rupture occurred during the 1946 Nankaido earthquake; i.e., brittle rupture in the eastern part and relatively slow slip in the western part. Studies on the effects of the buried seamont on the coupling between the plates [Kelleher and McCann, 1976, Scholz and Small, 1997] suggest that coupling between the subducted plate and the overriding plate becomes locally stronger due to the subduction of the seamont. From their conclusion [Scholz and Small, 1997], we propose that the seismo-tunamigenic brittle rupture starting off Kii peninsula turned landward at the Tosa-bae due to strong coupling at the large subducted seamont, then the slip might have propagated around the landward foot of the subducted seamont.

In segment D, from the seismic images described above, we conclude that a trough-parallel cyclic ridge subduction is now ongoing at the un-ruptured zone in the Tokai segment. The possibility of a subducted ridge (hereafter, referred to as the Paleo-Zenisu ridge) parallel to the Zenisu ridge has been suggested by previous studies on the basis of analog modeling, geomagnetic data, gravity data, and presence of sub-parallel old volcanic ridges (the Proto-Zenisu ridge) at the western flank of the Izu arc on the incoming plate [Le Pichon *et al.*, 1996; Lallemand, Malavieille and Calassou, 1992] (Fig. 1). Our survey successfully detected a seismic image of it, and showed that the subducted structure consists of a double ridge system, not a single ridge. The seismic images also show that the deeper Paleo-Zenisu ridge has been subducted beneath the back stop of the present day accretion process. The crustal block thickening toward land with a velocity of 4.5–5.5 km/s (between reflectors E and F) is interpreted as the old accretionary complex created before the opening of the Shikoku basin [Nakanishi *et al.*, 1998; Kodaira *et al.*, 2002], and it is considered to function as the back stop to accumulate sediments on the incoming plate [Nakanishi *et al.* 2002 d] As discussed by Nakanishi *et al.* [2002 d] we recognized that the back stop is moved landward where the ridge and the seamont are subducted (Fig. 1).

Comparing the deeper Paleo-Zenisu ridge with geodetic data [Sagiya, 1999] indicates that the ridge is located exactly beneath the area where the maxi-

mum back slip rate (landward moving velocity of the upper pate) is estimated by GPS data (Fig. 6). According to Sagiya [1999], a back slip rate of more than 35 mm/year, which is comparable to the plate convergent rate, is obtained about 50 km off-shore. This indicates nearly 100% locking (coupling) between the

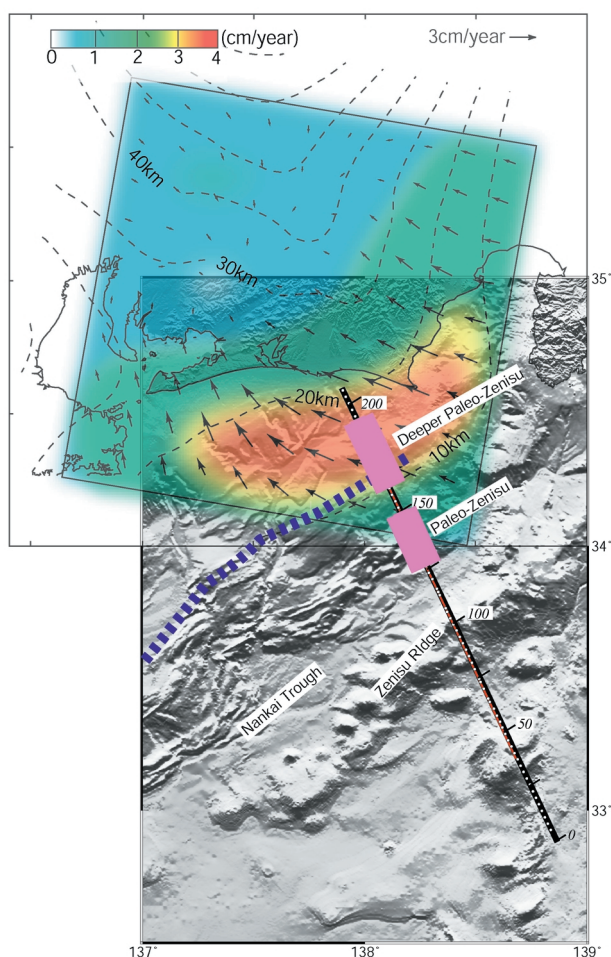


Fig. 6. Location of the cyclic ridge subduction and back slip distribution calculated from geodetic (GPS) data [Sagiya, 1999; Research group for active submarine faults off Tokai, 1999] Black and red lines indicate the wide-angle seismic refraction/reflection profile and near vertical seismic reflection profile, respectively [Kodaira *et al.* 2003]. White dots indicate OBS locations. Locations of the subducted deeper and the Paleo-Zenisu ridges are shown by thick pink lines. Blue dotted line shows the seaward end of the back stop [Nakanishi *et al.* 2002 d] (Fig. 1). Color map, arrows, and dotted contours show the back slip distribution, the back slip vectors, and the depth of the plate boundary used for calculating the back slip, respectively [Sagiya, 1999]. This figure clearly demonstrates that the deeper Paleo-Zenisu ridge is situated exactly at the inter-plate locked zone.

plates at the deeper Paleo-Zenisu ridge. Several geophysical studies have suggested strong coupling at the subducted seamount. For example, Scholz and Small [1997] deduced from earthquake activity and satellite gravity data that the subduction of a large seamount will increase the normal stress across the subduction interface and hence will enhance seismic coupling. Baba *et al.* [2001] estimated stress accumulation around the subducted seamount from a numerical simulation.

In conclusion, the high-resolution seismic images clearly demonstrate that the lateral extent of the rupture zones in the Nankai seismogenic zone is strongly controlled by the structures of the subducted oceanic crust; i.e., our study strongly suggests evidence of the subducted seamount — strongly locking hypothesis, where a large-scale ridge or seamount is subducted beneath a back stop in an accretion dominant subduction zone. The locked region may rupture when accumulated stress

exceeds the critical strength of locking. This could explain why the recurrence interval of the great earthquake in the Tokai segment is longer or more obscure than the other segments. We also propose that the subducted convex shape would not produce a strong coupling when the convex is located under young accretionary sediment, presumably a weaker material.

Acknowledgement

The main part of this study was done as a research program for plate dynamic in IFREE. We thank Dr. T. Tsuru, Dr. S. Miura, Dr. T. Hori, and A. Ito (IFREE) for their support and fruitful discussions on this study. We also thank Y. Kosumi for preparing the figures. Dr. R. Hino (Tohoku Univ.) and Dr. M. Shinohara (Univ. Tokyo) are acknowledged for giving us an opportunity to write this paper.

(Received February 22, 2003)

(Accepted July 15, 2003)